Optimal Operation of EV Charging Station Integrated Virtual Power Plant with Providing Frequency Regulation Services

Xiaotian Liu*, Jiawei Zhang, Cuo Zhang
School of Electrical and Computer Engineering
The University of Sydney
Sydney, Australia
*E-mail: xiaotian.liu@sydney.edu.au

***Abstract*—The increasing penetration of distributed energy resources presents both challenges and opportunities for system frequency control, necessitating advanced strategies for virtual power plants (VPPs). This paper proposes an optimal operation method for a VPP comprising photovoltaics (PVs), battery energy storage systems (BESSs), and an electric vehicle charging station (EVCS), to provide frequency regulation services (FRS) and maximize its profitability via energy management of BESS and EVCS. As a key contribution, a new model that determines the optimal power capacity for FRS by strategically scheduling the aggregated charging flexibility of EVs is proposed. To address the critical challenge of reliable service delivery under signal uncertainty, a robust BESS operational model employing a feasible region for state of charge (SoC) is developed. This new model can update boundaries of BESS operation, guaranteeing FRS commitments under any sequential response without violating physical limits and avoiding the suboptimal relying on conservative margins. Case studies demonstrate that the proposed method can efficiently enhance VPP revenues with guaranteed power capacity for FRS, highlighting the economic and technical benefits of integrating EVCS flexibility.**

***Keywords*—Electric vehicle charging station, frequency regulation, optimization, uncertainty, virtual power plant.**

I. Introduction

During recent years, modern power systems have been undergoing fundamental reshaping due to the rapid proliferation of distributed energy resources (DERs). This transformation is driven by the dual trends of increasing photovoltaic (PV) penetration on the generation side and escalating electric vehicle (EV) adoption on the demand side. While critical for decarbonization, the variability and uncertainty of DERs pose challenges to the stable and reliable operation of power system, necessitating effective frequency regulation services (FRS) to mitigate these risks [1]. To effectively integrate and control DERs, establishing and operating virtual power plants (VPPs) has been widely adopted. VPP can coordinate PVs, battery energy storage systems (BESS), and adjustable loads into a dispatch entity through information and communication technologies, enabling it to participate in energy and FRS markets, and improving the utilization rate of renewable energy [2].

In the literature, the potential of VPP to provide FRS is well-documented. In [3], a VPP provides FRS by coordinating wind power generators and BESSs. Based on this, [4] further considers the uncertainty of wind power and proposes a game-based model of VPP operation for both FRS and energy market. The work in [5] introduces a coordinated control strategy for a VPP consisting of distributed BESSs and water heaters. However, the primary enabler of the power capability for FRS, i.e., BESS, is often constrained by high capital investment, resulting in a relatively limited capacity within a VPP. Besides, keeping state of charge (SoC) for multiple purposes (energy shift and fast power response) is still a research challenge.

On the other hand, electric vehicle charging stations (EVCSs) emerge as pivotal aggregation hubs, capable of harnessing the latent flexibility of numerous individual EVs. By coordinating the charging processes of all connected EVs, an EVCS can modulate its aggregate power consumption in real time, allowing it to function as a virtual BESS, rapidly adjusting its charging curve [6]. Thus, the fast-response characteristics of a physical BESS can be formed for providing ancillary services like FRS. Ref. [7] proposes a multi-timescale frequency control strategy of VPP, involving EV charging piles. In [8], a stochastic scheduling approach that addresses multi-source uncertainty on integrated PV-BESS-EVCS systems is proposed. In [9], a hierarchical scheduling strategy under a cloud-edge framework for EV aggregators is designed to provide concurrent frequency and voltage regulation. In [10], an optimization method of VPP operation is proposed, considering EV clusters and the uncertainties of DERs for both energy and FRS markets.

While the existing work acknowledges the potential of VPPs in providing FRS, a clear methodology for how to optimally determine and reliably prepare an expected power capacity for FRS from integrated EVCS and BESS remains a significant research gap.

This paper proposes an optimal operation method for a VPP integrating an EVCS to enhance its participation in both energy

This work was supported in part by Australian Research Council under Grant DE240100059 and DP260101914.

979-8-3315-8138-1

and FRS markets. *A new optimization model of VPP operation utilizing EV charging flexibility for FRS* is proposed. It aims to maximize the total operational profits of a VPP considering both energy market and FRS provision. Furthermore, *a robust BESS model to securely prepare the power capacity for FRS* is proposed. A feasible region of SoC is introduced, guaranteeing operational safety under stochastic FRS request signals without conservative reservations, maximizing the utilization of BESS for both energy trading and FRS.

II. EVCS Integrated VPP For FRS

A. EVCS Integrated VPP Framework

The proposed VPP integrates distributed PV, BESS, and EVCS at the system level into a coordinated framework, achieving the collaborative optimization of flexible loads and renewable energy, as shown in Fig 1.

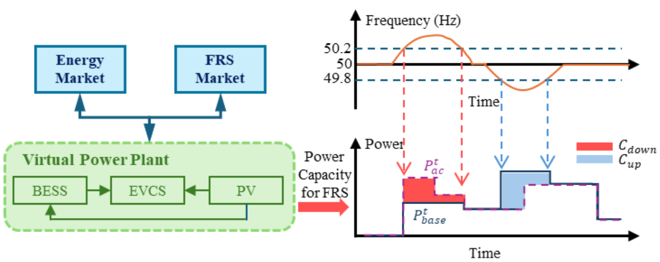

Figure 1. Overall structure of the proposed VPP system

This structure enables the VPP to achieve joint optimization of power purchase and sale, along with FRS while considering the uncertainty of request. P_t^{base} donates the baseline power generation of VPP at time t, presenting the working condition without FRS signal. P_t^{ac} is the power which is optimized to respond to FRS request signals. When frequency deviates out of the range, the real time power generation switches to P_t^{ac} from P_t^{base}, providing FRS.

As a main contribution, an optimization model is proposed to prepare the power capacity for FRS which can be activated to response to FRS request signals in real time.

B. Revenues from FRS

This paper presents the up/down FRS capacity based on the optimization problem of maximizing the revenue of the VPP. The difference between the baseline power curve and the response curve contributes to the capacity for FRS [11] as below.

$$max\{FRS\ revenues - operation\ cost\} \tag{1}$$

$$C_t^{up} = \Delta t\left(P_t^{base} - P_t^{ac}\right)\ \forall t \in T^{up} \tag{2}$$

$$C_t^{down} = \Delta t\left(P_t^{ac} - P_t^{base}\right)\ \forall t \in T^{down} \tag{3}$$

Here, T^{up} and T^{down} respectively represent the upward-regulation and downward-regulation time periods. Thus, the power capacity is unlocked by switching to the optimized response curve, contributing to the FRS revenues.

III. DER Operation Models

It is assumed that a VPP has PVs, BESSs and an EVCS, and their operation models are formulated in this section.

A. PV Operation Model

The PV generation describes the active power output of the photovoltaic units integrated into the VPP. The output power of photovoltaic at each time step t is limited by the maximum power [12] as follows.

$$0 \le p_t^{pv,base} \le p^{pv,max} \tag{4}$$

$$0 \le p_t^{pv,ac} \le p^{pv,max} \tag{5}$$

Here, $p_t^{pv,base}$ and $p_t^{pv,ac}$ denote PV power generation under baseline and response state, respectively, while $p^{pv,max}$ represents the rated maximum generation capacity of the PV system.

B. BESS Operation Model

The dynamic charging and discharging characteristics of the BESS in the VPP provides fundamental support for energy management and frequency regulation, constrained by both the baseline and the response trajectory. The model reflects the BESS actions in the baseline and response states as follows.

$$p_t^{ch} = (1-y_t)p_t^{ch,base} + y_t p_t^{ch,ac} \tag{6}$$

$$p_t^{dis} = (1-y_t)p_t^{dis,base} + y_t p_t^{dis,ac} \tag{7}$$

$$0 \le p_t^{ch} \le b_t p^{ch,max} \tag{8}$$

$$0 \le p_t^{dis} \le (1-b_t)p^{dis,max} \tag{9}$$

Here, p_{ch}^t and p_{dis}^t represent the expected power of BESS charging and discharging, respectively. The expected power is calculated using the FRS request signal y_t as the weight for optimization. When $y_t = 0$, the BESS power equals the baseline power. Otherwise, i.e. $y_t = 1$, it changes to the response trajectory, responding to the FRS signal during time T^{up} and T^{down}. $p^{ch,max}$ and $p^{dis,max}$ in (8) and (9) are the maximum power limits, and b_t is the binary parameter indicating charging or discharging at time t.

The traditional BESS scheduling for FRS uses conservative and fixed SoC margins to accommodate deviations from a planned trajectory caused by uncertain request signals below.

$$SoC_{t+1} = SoC_t + (\eta^{ch} p_t^{ch}\Delta t - p_t^{dis}\Delta t/\eta^{dis})/C \tag{10}$$

Here, η^{ch} and η^{dis} are charging and discharging efficiency and C is the rate capacity of BESS. Despite simplicity, this method is suboptimal as it unnecessarily restricts the BESS capacity. Moreover, fixed margin risks either SoC violations from extreme FRS request signals or crippled profitability.

This work proposes a concept of SoC feasible region that enables the upper and lower boundaries of SoC for each time step by considering both the baseline operation and the extreme FRS response scenarios, ensuring operational safety without sacrificing capacity. The change of SoC at time t highly depends on the FRS signal y_t based on (6) and (7) as follows.

$$\Delta SoC_t^{base} = (\eta^{ch} p_t^{ch,base}\Delta t - p_t^{dis,base}\Delta t/\eta^{dis})/C \tag{11}$$

$$\Delta SoC_t^{ac} = (\eta^{ch} p_t^{ch,ac}\Delta t - p_t^{dis,ac}\Delta t/\eta^{dis})/C \tag{12}$$

Here, upper and lower limits of the SoC feasible region of the baseline curve are shown in (13) and (14) while the limits of response trajectory are shown in (15) and (16) as follows.

979-8-3315-8138-1

$$L(t+1) \leq L(t) + \Delta SoC_t^{base}\ \forall y_t = 0 \tag{13}$$

$$U(t+1) \geq U(t) + \Delta SoC_t^{base}\ \forall y_t = 0 \tag{14}$$

$$L(t+1) \leq L(t) + \Delta SoC_t^{ac}\ \forall y_t = 1 \tag{15}$$

$$U(t+1) \geq U(t) + \Delta SoC_t^{ac}\ \forall y_t = 1 \tag{16}$$

At time $t+1$, if there is no FRS request signal, the battery operates according to the baseline, corresponding to (11). Otherwise, the change of SoC is formulated by (12). The maximum value of SoC that BESS can reach at time $t+1$ is the sum of SoC_t and the maximum of ΔSoC_t^{base} and ΔSoC_t^{ac} as follows.

$$L(t+1) \leq max\{L(t) + \Delta SoC_t^{base}, L(t) + \Delta SoC_t^{ac}\}\ \forall t \tag{17}$$

$$U(t+1) \geq max\{U(t) + \Delta SoC_t^{base}, U(t) + \Delta SoC_t^{ac}\}\ \forall t \tag{18}$$

This model comprehensively depicts the dynamic operation characteristics of the BESS in VPP, allows SoC_t for all time intervals to fall within the feasible region of $[L(t), U(t)]$, guarantees operational safety while maximizing the capacity.

C. EVCS Operation Model

The EVCS model is used to describe the charging behaviors of a single EV and the aggregated power characteristics [12] of the entire charging station within a VPP. This model considers the arrival and departure time of each EV, the power limit of individual charging points, and the overall capacity constraints of the charging station. Additionally, the model strives to ensure that each EV completes required charging demand within the available connection time window, while enabling the overall load of the EVCS to respond to FRS signals. The mathematical model established in this section provides the operational basis for integrating EVCS into the VPP collaborative optimization framework. The connection status of vehicle m at time t is represented by a binary variable $\alpha_{m,t}$ as follows.

$$\alpha_{m,t} = \{0,1\}\ \forall\ t \in [T_m^{arr}, T_m^{dep}] \tag{19}$$

$$\alpha_{m,t} = \{0\}\ \forall\ t \notin [T_m^{arr}, T_m^{dep}] \tag{20}$$

Here, T_m^{arr} and T_m^{dep} represent the arrival and departure times of vehicle m. When $\alpha_{m,t} = 1$, it indicates EV m is connected to station and can be charged; otherwise, it represents an unconnected state. The charging power of each EV is limited by the maximum allowable power p_m^{max}, for both the baseline state $p_{m,t}^{base}$ and response state $p_{m,t}^{ac}$, where y_t is the request signal as shown in (6) and (7) and $p_m^{EV,max}$ is the maximum allowable power of each EV m as follows.

$$0 \leq (1-y_t)p_{m,t}^{base} + y_t p_{m,t}^{ac} \leq \alpha_{m,t} p_m^{EV,max} \tag{21}$$

The total power of EVCS is equal to the sum of the charging power of all the vehicles that are currently being charged below.

$$p_t^{EVCS} = \sum_m \left[(1-y_t)p_{m,t}^{base} + y^t p_{m,t}^{ac}\right] \tag{22}$$

Before each EV departs, energy demand needs to be satisfied. However, to respond to the FRS signal, some energy may be cut down, which are constrained as follows.

$$\sum_{t=T_m^{arr}}^{T_m^{dep}} \left[(1-y_t)p_{m,t}^{base} + y_t p_{m,t}^{ac}\right]\Delta t + s_m \geq E_m^{req} \tag{23}$$

$$s_m \geq 0 \tag{24}$$

Here, E_m^{req} is the energy demand of vehicle m and s_m is a slack variable representing the energy gap that vehicle m still needs to meet after the charging process is completed. This constraint ensures that each EV can obtain the necessary energy within the charging window.

IV. Optimization of VPP Operation

A. Power Capacity for FRS

The FRS model describes the operational characteristics of capacity reservation and real-time activation, contributes to the stability of the system frequency by adjusting the power of PV, BESS and EVCS. The model focuses on the switching relationship between baseline power and FRS response power while guaranteeing the power balance constraints during both normal operation and FRS response phases, ensuring physical feasibility and compliance with the operating norms of Australian National Electricity Market (AEMO) as follows.

$$P_t^{buy} - P_t^{sell} = (1-y_t)P_t^{base} + y_t P_t^{ac} \tag{25}$$

Here, P_t^{sell} and P_t^{buy} respectively denote the power that the VPP sells and purchases at time t. Combining each DER, the baseline and response power profiles of the VPP described in (2) and (3) and are reformulated as follows.

$$P_t^{base} = p_t^{ch,base} + p_t^{EVCS,base} - p_t^{dis,base} - p_t^{pv,base}, \forall t \tag{26}$$

$$\begin{gathered} P_t^{ac} = p_t^{ch,ac} + p_t^{EVCS,ac} - p_t^{dis,ac} - p_t^{pv,ac}, \\ \forall t \in (T^{up} \cup T^{down}) \end{gathered} \tag{27}$$

B. Optimization Model

The objective of this study is to maximize the expected total revenue of the VPP in the energy market and the FRS market. Within the scheduling period, the VPP achieves revenue from power purchase and sale transactions, capacity backup, and frequency regulation through the coordinated operation of PV, BESS, and EVCS. Meanwhile, penalty costs resulting from charging demand defaults are also taken into consideration. The MILP problem of the VPP operation is formulated below.

$$max \sum_{t \in T} R^{grid} + R^{FRS,res} + R^{FRS,ac} + R^{EVCS} - Penalty \tag{28}$$

subject to:

$$R^{grid} = \sum_{t=1}^{T} \left(\pi_t^{sell} P_t^{sell} - \pi_t^{buy} P_t^{buy}\right)\Delta t \tag{29}$$

$$R^{FRS,res} = \sum_{t=1}^{T} \pi_t^{res}\left(C_t^{up} + C_t^{down}\right) \tag{30}$$

$$R^{FRS,ac} = \sum_{t=1}^{T} y_t \pi_t^{ac}\left(C_t^{up} + C_t^{down}\right) \tag{31}$$

$$R^{EVCS} = \sum_{t=1}^{T} \pi_t^{EVCS} p_t^{EVCS} \Delta t \tag{32}$$

$$Penalty = c_{slack} \sum_{m=1}^{n} s_m \tag{33}$$

$$\text{(4)-(27)} \tag{34}$$

Herein, π_t^{sell} and π_t^{buy} represent the time-of-use electricity prices for selling and buying at time t. $R^{FRS,res}$ donates the compensation received by the VPP for the reserved capacity reported to the FRS market, and $R^{FRS,ac}$ denotes the revenue from FRS supported by the VPP. Besides, π_t^{res} and π_t^{ac} are the prices for reserve capacity and activated FRS capacity. C_t^{up} and C_t^{down} are calculated from (2)-(3) and (26)-(27).

The revenue from EVCS, R^{EVCS}, is the summation of service fee π_t^{EVCS} times charging power over the whole period. However, by actively curtailing the energy demand of some EVs during the upward-regulation period, the VPP can increase the available capacity for FRS, thereby maximizing the potential revenue. Thus, the penalty coefficient c_{slack} is introduced, indicating the negative impact of s_m in (24).

V. Case Study

A. Simulation Parameter Settings

1) FRS Request Signal Setting

For request signals setting, the overall process follows a frequency regulation time window. If a frequency modulation signal occurs within the upward-regulation time window, it is identified as an upward-regulation signal; conversely, if it occurs outside this time window, it is regarded as a downward-regulation signal. In this paper, the frequency modulation window time is set to approximately half of the middle point as the high-probability activation time for FRS. The specific period and probability settings are given in TABLE I.

TABLE I. Activation Period and Probability of FRS

FRS Type	Time Period	Request Probability
Upward-Regulation	6:30–7:30	0.4
	17:00–21:00	0.55
Downward-Regulation	00:00-6:00	0.01
	12:00–14:00	0.45
Others	Other times	0.01

2) Energy and FRS Market Prices

The grid electricity price π_t^{sell} and π_t^{buy} are based on the actual electricity price in New South Wales, from AEMO [14]. The specific price of the 5-minute resolution FRS has not been found in public information. This work assumes the reserve price to be 0.01 AUD/kWh while the FRS price is set at 0.8 AUD/kWh, slightly higher than the electricity price.

3) EVCS Charging Prices and Vehicle Scheduling

The price of EVCS charging is based on Tesla charging stations [15]. This study adopts a time-of-use electricity price of 0.66 AUD/kWh for peak hours (10:00–20:00) and 0.42 AUD/kWh for off-peak hours, based on market data. The average daily power consumption per charging stall is 251 kWh [16], and each charging stall charges 7 vehicles per day. For the simulation, the daily vehicle throughput for each charging stall is set to 10. Referring to Tesla "Model" series [17] and usage patterns, this study set the EV energy demand to average 36 kWh (ranging 20-65 kWh), aligning with real-world patterns. EV arrival and departure data is generated using a multi-peak distribution to emulate realistic urban charging patterns, including workplace and commuter charging peaks.

B. Optimization Results

This paper generates three cases to highlight the effects of the participation of EVCS for FRS market. Optimization and numerical simulations are conducted with 5-minute-interval on MATLAB using YALMIP and solved by CPLEX [18].

1) Case 1: BESS + Curtailable PV

In this case, the VPP has no EVCS while the PV energy is curtailable. The optimized power capacity is shown in Fig 2. The VPP provides limited upward-regulation capacity in the absence of EVCS integration.

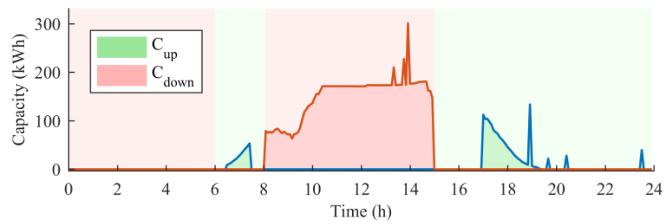

Figure 2. Optimized power capacity for Case 1

2) Case 2: BESS + Non-curtailable PV + EVCS

This case enables the integration of EVCS, with Non-curtailable PV, as in Fig 3. The upward-regulation capacity increases significantly due to the scheduling of EVs.

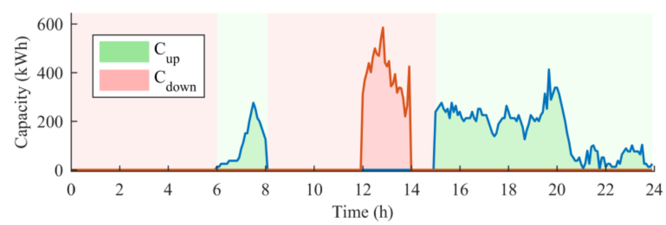

Figure 3. Optimized power capacity for Case 2

3) Case 3: BESS + Curtailable PV + EVCS

Compared to Case 2, this Case demonstrates that by allowing PV curtailment, the VPP offers additional downward-regulation power capacity without compromising the predetermined EVCS dispatch schedule, as shown in Fig 4.

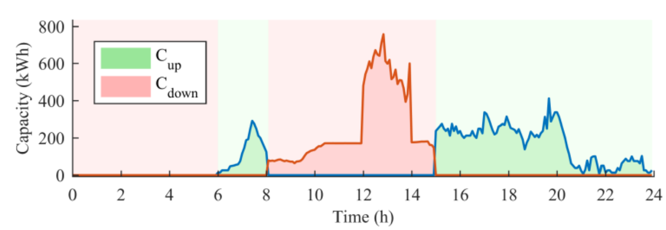

Figure 4. Optimized power capacity for Case 3

The comparison of the maximum available FRS capacity of each case is presented in Fig 5.

979-8-3315-8138-1

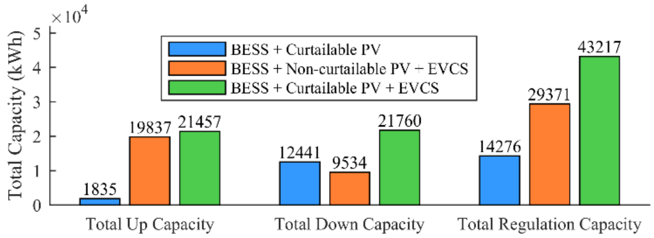

Figure 5. Comparison of power capacity for FRS

The optimization results of three cases indicate the integration of the EVCS can significantly enhance the total power capacity for FRS. By rescheduling the charging requirement of each aggregated EV, the VPP unlocks substantial upward-regulation capacity. It is noted the PV curtailment means consuming more power, contributing to downward-regulation capacity.

C. Real-Time Validation

Considering the uncertainty of FRS request signals, this paper conducts Monte Carlo simulation with 10,000 realization scenarios generated based on TABLE I. to test the robustness of each model under random FRS response. The average revenue is given in TABLE II.

TABLE II. ACTIVATION PERIOD AND PROBABILITY OF FRS

Revenue Item	Case 1	Case 2	Case 3
Grid Trading ($)	3413.05	-1265.99	-1704.57
FRS Reserve ($)	142.76	293.71	432.17
FRS Response ($)	2390.44	8187.74	10433.77
EVCS Charging ($)	NA	18868.76	18876.33
Penalty ($)	NA	-246.04	-245.61
Total ($)	5946.26	25838.17	27792.08

The negative sign of grid trading means the VPP purchases power from the main grid. While the integration of EVCS leads to purchasing power from the grid, it contributes more profits to the VPP. Although allowing PVs to participate in FRS by curtailing its power generation slightly increases electricity purchase costs, the resulting FRS revenue gains lead to a 7% increase in the total profit, validating the superior economic performance of the proposed model.

It is notable that the application of the SoC feasible region corresponding to (13)-(18) ensures the robust performance validated by the Monte Carlo simulation. Sufficient BESS SoC is maintained, and no constraint violations are observed.

VI. CONCLUSION AND FUTURE WORK

This paper presented an optimal operation strategy for a VPP integrating an EVCS to co-optimize its participation in energy and FCAS markets. The proposed method calculates the optimal FRS capacity by leveraging the aggregated flexibility of EVs. Critically, a robust BESS model with feasible region is developed to securely prepare this capacity. This ensures that the BESS can reliably provide FRS under real-time uncertainty without violating physical limits, overcoming the limitations of conservative, static margins. Case studies validated the approach enhances the profitability and flexibility of the VPP, maximizing market value.

In future work, the proposed VPP operational model can be extended for a broader system context with consideration of network operating constraints such as bus voltage limits. Besides, the coordination and competitive dynamics among multiple VPPs can be considered and addressed regarding their collective impacts on power system operation and energy market.

REFERENCES

[1] H. Golpîra and B. Marinescu, "Enhanced Frequency Regulation Scheme: An Online Paradigm for Dynamic Virtual Power Plant Integration," *IEEE Trans. Power Systems*, vol. 39, no. 6, pp. 7227-7239, Nov. 2024.

[2] X. Li, C. Yip, Z. Y. Dong, C. Zhang, and B. Wang, "Hierarchical control on EV charging stations with ancillary service functions for PV hosting capacity maximization in unbalanced distribution networks," *Int. J. Electr. Power Energy Syst.*, vol. 160, p. 110097, 2024.

[3] G. He, Q. Chen, C. Kang, et. al., "Cooperation of wind power and battery storage to provide frequency regulation in power markets," *IEEE Trans. Power Syst.*, vol. 32, no. 5, pp. 3559–3568, Sep. 2017.

[4] W. Chen, J. Qiu, J. Zhao, Q. Chai and Z. Y. Dong, "Bargaining Game-Based Profit Allocation of Virtual Power Plant in Frequency Regulation Market Considering Battery Cycle Life," *IEEE Trans. Smart Grid*, vol. 12, no. 4, pp. 2913-2928, July. 2021

[5] A Oshnoei, et al., "Coordinated control scheme for provision of frequency regulation service by virtual power plants." *Applied Energy*, vol. 325, 119734, 2022.

[6] H. Wang, Y. Jia, M. Shi, et. al., "A mutually beneficial operation framework for virtual power plants and electric vehicle charging stations," *IEEE Trans. Smart Grid*, vol. 14, no. 6, pp. 4634–4648, Nov. 2023.

[7] L. Mo, et. al., "Multi-Time Scale Frequency Regulation Control of Virtual Power Plant Based on Fuzzy Sets," *IEEE Trans. Smart Grid*, vol. 16, no. 3, pp. 2361-2374, May 2025.

[8] X. Dong, Y. Guo, M. Li, et. al., "Stochastic optimization of integrated electric vehicle charging stations under photovoltaic uncertainty and battery power constraints," *Energy*, vol. 314, p. 134163, Jan. 2025.

[9] X. Lu and L. Wang, "Cloud-Edge Collaboration Control Strategy for Electric Vehicle Aggregators Participating in Frequency and Voltage Regulation," *IEEE Open Journal of Vehicular Technology*, vol. 5, pp. 1532-1544, 2024.

[10] W. Qin, X. Li, X. Jing, Z. Zhu, R. Lu and X. Han, "Multi-Temporal Optimization of Virtual Power Plant in Energy-Frequency Regulation Market Under Uncertainties," *Journal of Modern Power Systems and Clean Energy*, vol. 13, no. 2, pp. 675-687, March 2025.

[11] H. Saberi, C. Zhang, and Z. Y. Dong, "Capacity of virtual energy storage system for frequency regulation services via a data-driven distributionally robust optimization method," *IEEE Trans. Power System.*, vol. 38, no. 3, pp. 2134–2146, May 2023.

[12] Q. Meng, S. Hussain, F. Luo, Z. Wang and X. Jin, "An Online Reinforcement Learning-Based Energy Management Strategy for Microgrids with Centralized Control," *IEEE Trans. Industry Applications*, vol. 61, no. 1, pp. 1501-1510, Jan.-Feb. 2025.

[13] A. Hafeez, R. Alammari and A. Iqbal, "Utilization of EV Charging Station in Demand Side Management Using Deep Learning Method," *IEEE Access*, vol. 11, pp. 8747-8760, 2023.

[14] AEMO. [Online]. Available: https://www.aemo.com.au.

[15] D. Bleakley, "Tesla offering big discounts for off-peak Supercharging at some locations," The Driven, Jun. 16, 2023. [Online]. Available: https://thedriven.io/2023/06/16/tesla-offering-big-discounts-for-off-peak-supercharging-at-some-locations/.

[16] K. Kane, "Tesla Supercharging Network: Q2 2025 Report," EVChargingStations.com, Jul. 24, 2025. [Online]. Available: https://evchargingstations.com/chargingnews/tesla-supercharging-network-q2-2025-report/?utm_source=chatgpt.com.

[17] Tesla, Inc., [Online]. Available: https://www.tesla.com/en_au.

[18] Int. Bus. Mach., "User's Manual for CPLEX", [Online]. Available: https://www.ibm.com/docs/en/icos/22.1.1?topic=optimizers-users-manual-cplex.